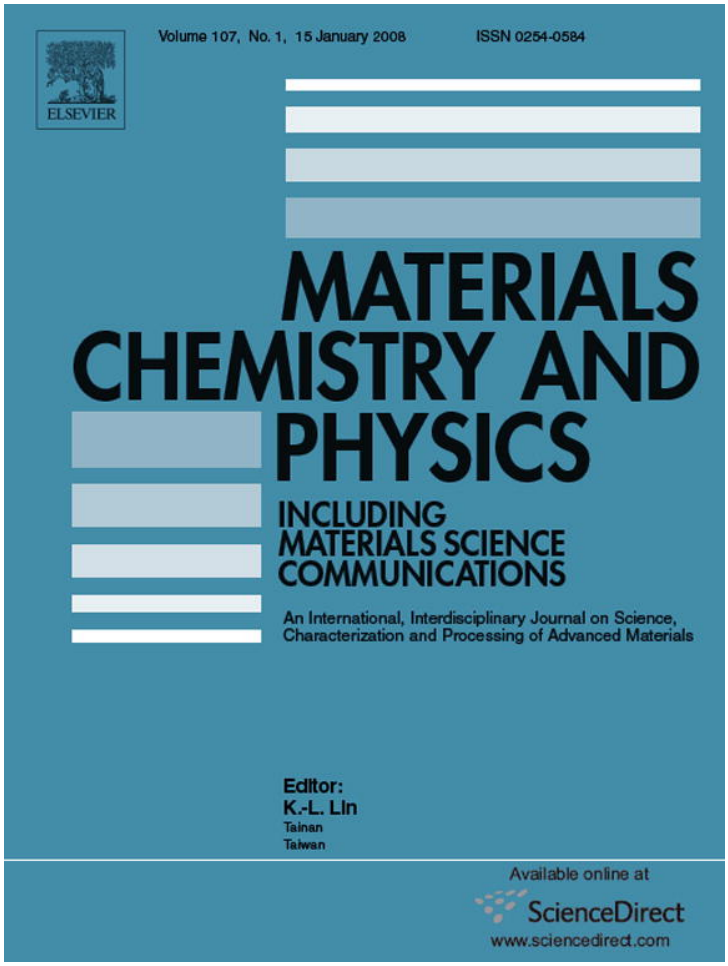

Available online at www.sciencedirect.com
ScienceDirect
Materials Chemistry and Physics 107 (2008) 148–152
MATERIALS CHEMISTRY AND PHYSICS
www.elsevier.com/locate/matchemphys

Wear and corrosion resistant coatings formed by microarc oxidation on TiAl alloy

Xi-Jin Li [a], Guo-An Cheng [a,b,*], Wen-Bin Xue [a,b], Rui-Ting Zheng [a,b], Yun-Jun Cheng [c]

[a] *Key Laboratory of Beam Technology and Material Modification of Ministry of Education, Department of Materials Science & Engineering, Beijing Normal University, Beijing 100875, PR China*
[b] *Institute of Low Energy Nuclear Physics, Beijing Normal University, Beijing 100875, PR China*
[c] *Research Center of Ti-Al Intermetallic Compound, High Temperature Material Research Division, General Iron & Steel Research Institute, Beijing 100081, PR China*

Received 16 January 2007; received in revised form 23 June 2007; accepted 28 June 2007

Abstract

Microarc oxidation is an advanced method to fabricate ceramic coatings on valve metals. The coatings up to 110 μm thick were prepared on γ-TiAl alloy by the alternating-current microarc oxidation in silicate electrolyte. Their structures, composition, wear resistance and corrosion resistance were evaluated by scanning electron microscopy (SEM), X-ray diffraction (XRD), ball-disc dry sliding and electrochemical polarization tests. Results showed that the dense layer of coatings was mainly composed of Al_2TiO_5 and TiO_2 rutile phases, while the loose layer contained a large amount of amorphous SiO_2 besides Al_2TiO_5 and TiO_2 rutile phases. Maximum value of microhardness in the coating was about three times higher than that of TiAl substrate. The wear rate of coating was only 1/10 of TiAl substrate. Corrosion current density of the coated TiAl alloy was greatly reduced. The microarc oxidation is a promising method to improve the wear resistance and corrosion resistance of TiAl alloy.

Keywords: Microarc oxidation; TiAl; Tribology; Corrosion resistance

1. Introduction

TiAl alloys attracted more attention in many fields due to their high specific strength, high melting point and excellent corrosion resistance, such as important parts of rocket, automobile, aeroplane and space shuttle. However, many properties of TiAl alloy should been further promoted in most of applied fields. A series of surface modification techniques, such as ion implantation [1], titanizing [2], and MCrAlY composite coating [3] have been developed to improve properties of TiAl alloys. Microarc oxidation (MAO) is a distinguished technique to fabricate a ceramic coating on light alloys due to the following advantages: (a) an excellent adhesion between coating and substrate because of in situ growth of ceramic coating, as metal ions coming from substrate and oxygen ions coming from electrolyte; (b) low cost, as this technique has no need of costly vacuum or gas shielding conditions; (c) easy controlling for processing, as coating can be easy controlled by electronic parameters and composition of electrolyte; (d) friendly for environment, as alkaline electrolytes were employed in the process [4–15]. Especially, MAO method enabling to achieve more thick ceramic coatings with high hardness, good wear resistance has shown a widely applied prospect [15–20].

At present, many papers about MAO were focused on the treatments of Al, Ti and Mg [10–17]. However, few data can be available concerning on fabricating the ceramic coatings on TiAl alloys by microarc oxidation technique [21]. Specially, no paper has been reported on tribological properties and corrosion resistance of MAO coating on TiAl substrate. In this work, structure and composition of MAO coatings on TiAl alloy were analyzed, and tribological and corrosive behaviors of the coatings were evaluated.

2. Experimental details

A γ-TiAl alloy with nominal composition of (at.%) 48Al, 2Cr and 2Nb was used as the raw material. The uncoated samples with a size of

* Corresponding author at: Key Laboratory of Beam Technology and Material Modification of Ministry of Education, Department of Materials Science & Engineering, Beijing Normal University, Beijing 100875, PR China.
Tel.: +86 1062205403; fax: +86 1062205403.
E-mail address: gacheng@bnu.edu.cn (G.-A. Cheng).

0254-0584/$ – see front matter © 2007 Elsevier B.V. All rights reserved.
doi:10.1016/j.matchemphys.2007.06.067

18 mm × 12 mm × 3 mm were polished up to 600# emery paper. An alternating-current power supply with 30 kW was employed to fabricate MAO coatings on TiAl alloy. The electrolyte was prepared with a solution of Na_2SiO_3 and KOH in distilled water. During MAO processing, the solution temperature was kept at below 50 °C. After 120 min MAO treatment, the coating thickness on TiAl alloy reached about 110 μm, measured by an eddy-current thickness gauge. After the loose outer layers were polished off, the inner layers with thickness of 20 μm and 50 μm were left, respectively. The alloy substrate and the samples of 20 μm and 50 μm rest thickness for tribological test were designated as samples 1#, 2#, 3#, respectively.

The cross-sectional microstructure of coating was investigated using a Siron 200 scanning electron microscopy (SEM). The composition profiles across coatings were analyzed by energy dispersive X-ray spectrum (EDX). X-ray diffraction (XRD) was carried out using an X' PERT PRO MPD X-ray diffractometer to determine phase constituents in the coatings. Microhardness tester (HV1000) was employed to measure the hardness profile of the coating. The applied load is 10 g.

A GCr15 bearing steel ball with 10 mm diameter was used as couple material against MAO coating using a SRV ball-disc friction and wear tester under dry sliding. During wear test, a 5 N load and 24,000 cycles at ambient temperature was chosen. The friction coefficient was recorded. Then the wear rate, wear volume per load and sliding distance, was calculated from the wear grooves using Talysurf 5P-120 (Rank Taylor Hobson Co. Holand) profile-meter.

Potentiodynamic polarizing curves in 3.5% NaCl solution were measured using a CS300UA electrochemical workstation to evaluate corrosion behaviors before and after microarc oxidation on TiAl alloy. A three-electrode cell, with sample as working electrode, saturated calomel electrode (SCE) as reference electrode and platinum coil as counter electrode, was employed in this test. After 5-min initial delay, scan was conducted at a rate of 1 mV s^{-1} from −250 mV versus open circuit potential towards more noble direction.

3. Results and discussion

3.1. Microstructures of MAO ceramic coatings

Microstructure of coating was shown in Fig. 1(a). The average thickness of coating was about 110 μm, which was consistent with the result measured by eddy-current thickness gauge. The Ti, Al, Si element profiles across the coating were also indicated in Fig. 1(b). From Fig. 1, it can be displayed that there are three different areas in the coating according to the cross-sectional morphology and profiles of Ti, Al, Si elements. This implied that there were three layers in the coating: a dense inner layer (area II), an intermediate layer (area III) and a loose outer layer (area IV). The thicknesses of both dense layer and loose layer were about 30 μm, respectively.

From coating surface to alloy substrate, Al and Ti contents increased, while the change of Si content was reverse to Al and Ti contents. The Si content in the intermediate layer was lower than in the loose outer layer, and was not detected in the inner dense layer (see Fig. 1(b)). This was attributed to that element Al and Ti in the coating came from TiAl alloy substrate, and element Si was from the silicate electrolyte. As shown in Fig. 1(a), the inner layer was compact and pores were rarely observed. It might be assumed that Si ions mainly diffused into coating through discharge channel and form silicon dioxide during microarc oxidation. Therefore, the porous loose layer contained lots of SiO_2, while the Si element was rarely detected in the compact inner layer.

Distributions of Al, O and Ti contents in looser layer were completely different with that in dense layer. The high Si content appeared in loose layer, but only low Ti content was detected in this layer. It implied that the element contents in loose layer could be adjusted when electrolyte solution was changed, but compositions in dense layer were rarely affected by the electrolyte.

3.2. Phase constituents in MAO coatings

The phase constituents in the coating and substrate were determined by XRD (see Fig. 2). When the outer layer was polished off, only the 35 μm dense layer was left. Fig. 2 indicated that the phase constituents in MAO coating were completely different from TiAl substrate. The Al_2TiO_5 and TiO_2 rutile phases were obtained both in the loose layer and dense layer (see Fig. 2(b) and (c)). The diffraction peaks in Fig. 2(c) were sharp and very clear. But in Fig. 2(b), an amorphous broad peak at the 2θ below 40° besides the diffraction peaks of Al_2TiO_5 and TiO_2 rutile phases could be observed. The Si profile in Fig. 1(b) has identified that there was a large amount of Si element in the outer layer of coating. Those indicated that amorphous SiO_2 existed in the outer layer including the loose and intermediate layers.

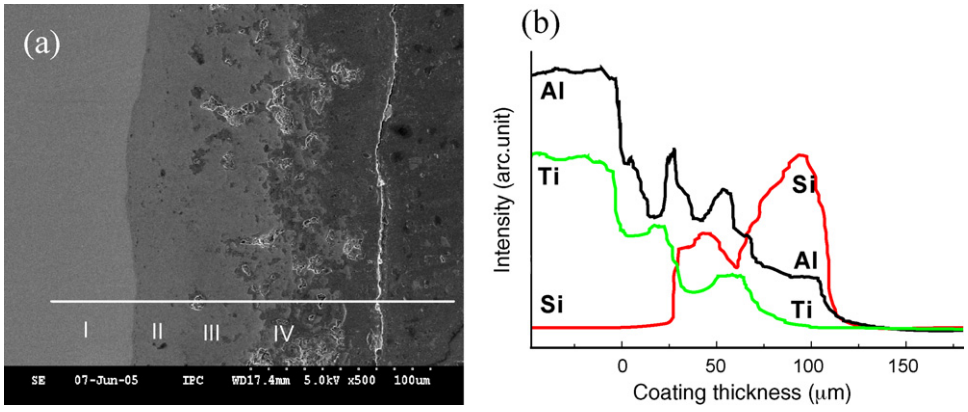

Fig. 1. Microstructure (a) and elements profiles (b) of MAO coatings for 120 min treatment (I) TiAl substrate; (II) dense layer; (III) intermediate layer and (IV) loose layer.

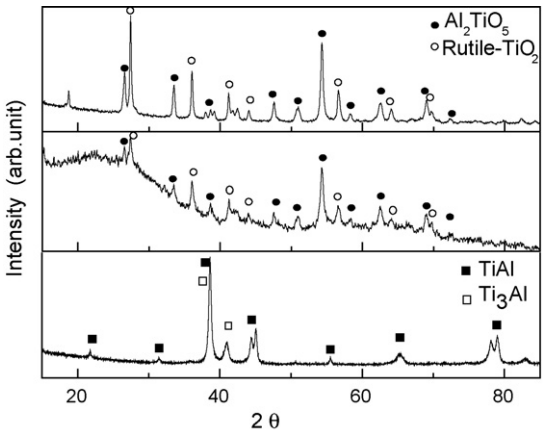

Fig. 2. XRD patterns for: (a) substrate; (b) MAO coating of 120 min treatment; (c) dense layer of (b).

3.3. Microhardness profile in MAO coatings

Fig. 3 showed that the microhardness of MAO coating gradually increased from outer surface of coating to the coating/substrate interface. The maximum hardness value of 13.5 GPa in MAO coating, located at about 10 μm away from the coating/substrate interface, was three times higher than in TiAl substrate. It was believed that a different phase composition and microstructure affected the microhardness of coating. Firstly, the inner layer was more compact than the outer layer, and the pore density decreased from outer layer to inner layer in MAO coating (see Fig. 1). So the microhardness of MAO coating gradually increased from coating surface to interior of coating. On the other hand, the dense layer consisted of only hard Al_2TiO_5 and TiO_2 rutile phases, which resulted in a higher hardness in the dense layer.

The layered structure in MAO coating was also identified by the microhardness profile. There were three layers to be observed from the microhardness profile, which was consistent with the morphology result in Fig. 1. According to the microhardness profile in Fig. 3, the area II, area III and area IV corresponded to the dense layer, intermediate layer and loose layer in MAO coating, respectively.

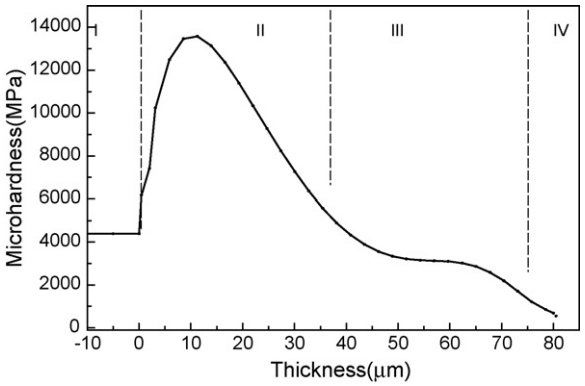

Fig. 3. Microhardness profile for 120 min microarc oxidation coatings.

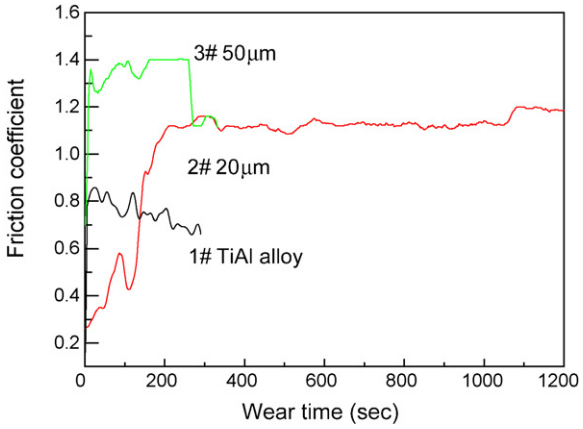

Fig. 4. Variation of friction coefficient with sliding distance (load: 5 N, frequency: 20 Hz).

3.4. Tribological properties of MAO coatings

Fig. 4 showed a variation of friction coefficient (μ) versus sliding distance on TiAl substrate and the polished coatings, respectively. For TiAl substrate (marked as sample 1#), the μ reduced gradually with increasing wearing time from 0.85 to 0.68. The μ of sample 2# with a rest thickness of 20 μm gradually increased from 0.30 to 1.12 within the initial 200 s, and then almost kept a constant of 1.12 after 200 s test. For the sample 3# with a rest thickness of 50 μm, the initial μ was about 1.40, which was higher than that for the sample 2#. When wearing time was more than 270 s, the μ of sample 3# was almost equal to that of sample 2#. Fig. 3 also showed that the hardness of MAO coating at 50 μm thickness away from the coating/alloy interface was much lower than that at 20 μm thickness. Moreover, as shown in Fig. 1, the porosity of MAO coating at 50 μm away from the coating/alloy interface was much higher than at 20 μm thickness. It resulted in higher friction coefficient for the coating with 50 μm rest thickness under dry sliding testing. When the surface layer was worn off, the μ was suddenly decreased to that of MAO coating with 20 μm rest thickness.

The wear tracks profiles of 1#, 2#, 3# samples were depicted in Fig. 5. Although the wear time of sample 2# was much

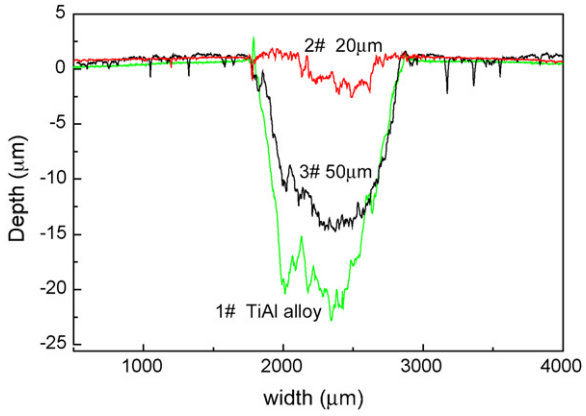

Fig. 5. Wearing track profiles of TiAl substrate and the MAO coatings polished to different thickness.

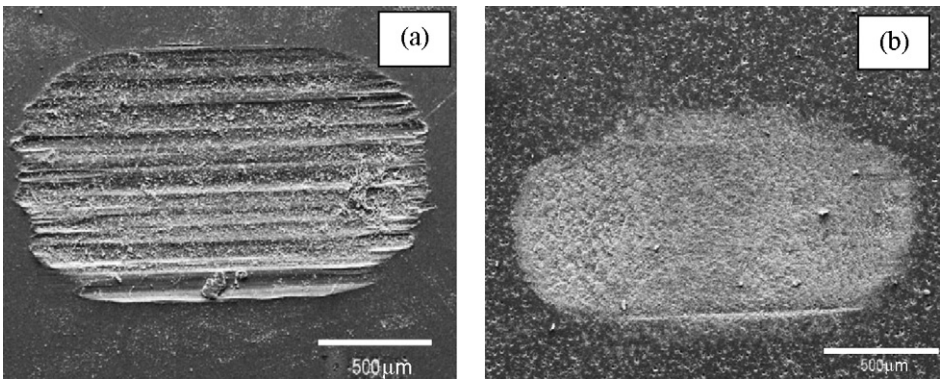

Fig. 6. The trace of wear surface: (a) substrate; (b) 20 μm polished coating.

longer than sample 1#, the track depth of sample 2# was smaller than sample 1#. The cross-sectional areas of wear tracks were obtained from Fig. 5 and then their wear rates could be calculated. The wearing rates of three samples of 1#, 3#, 2# were 27.0, 19.5 and 2.7 $mm^3\ N^{-1}\ m^{-1}$, respectively. The wear rate of the sample 2# was only 1/10 of that of sample 1#. As described in Fig. 3, the hardness of MAO coating at 20 μm away from interface of coating/substrate was much higher than that of TiAl substrate. Furthermore, Fig. 3 indicated that phases in the dense layer of MAO coating consisted of Al_2TiO_5 and TiO_2 rutile crystalline phases with high hardness. The dense microstructure and appearance of high-hardness phases of Al_2TiO_5 and TiO_2 rutile in the coating would cause a decrease of wear rate. Therefore, the wear rate of sample 2# with 20 μm rest thickness was lower than that of sample 3# with 50 μm rest thickness, and much lower than that of TiAl substrate.

After dry sliding, the morphologies of wear traces on sample 1# and sample 2# were observed (see Fig. 6). The depth of wear trace on TiAl substrate (Fig. 6(a)) was obviously deeper than that on MAO coating (Fig. 6(b)). That is consistent with the surface profile of wear trace in Fig. 5. Although the μ of MAO coating during dry sliding test was higher than that of TiAl substrate, the wear rate of MAO coating was much lower than that of TiAl substrate. Therefore, MAO coating could improve the wear resistance of TiAl alloy. Meanwhile, it implies that it is necessary to apply lubricants or other methods to reduce friction coefficient of MAO coatings on TiAl alloy.

3.5. Corrosion resistance of MAO coatings

Potentiodynamic polarization curves of bare and coated TiAl alloys were given in Fig. 7. Comparing curve *a* with curve *b*, the corrosion current density of 110 μm coating with $1.27 \times 10^{-9}\ A\ cm^{-2}$ was two orders of magnitude lower than that of TiAl substrate with $1.27 \times 10^{-7}\ A\ cm^{-2}$. The corrosion potential of MAO coating was about 100 mV more negative than that of TiAl substrate. However, comparing to the corrosion potential, the influence of corrosion current on suppressing the corrosion process was more important, therefore, the MAO treatment could improve the corrosion resistance of TiAl alloy.

From Fig. 1, it was indicated that there were some pores in outer layer of MAO coating. However, the MAO coating close to coating/substrate interface was compact and pores was rarely observed, which hindered the ions in the solution into the TiAl substrate. Meanwhile, the dense layer consisted of Al_2TiO_5 and TiO_2 which had a good stability against corrosion. Therefore, the corrosion resistance of coated TiAl alloy by MAO treatment was improved.

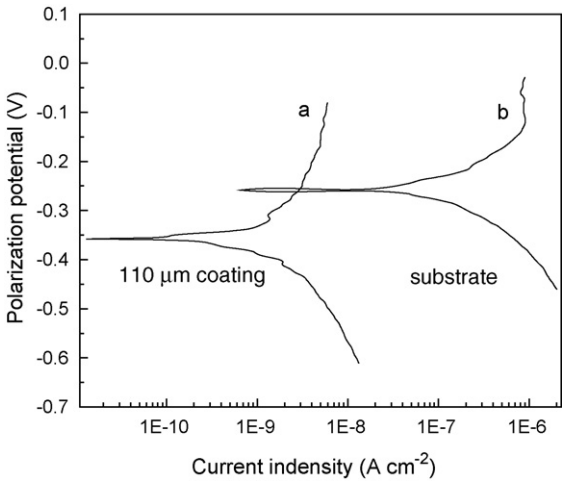

Fig. 7. Polarization curve of the MAO coating and the TiAl substrate (scanning rate 1 mv s^{-1}).

4. Conclusions

(1) The ceramic coating up to 110 μm had been prepared on TiAl alloy by MAO treatment. MAO coating consisted of three layers: dense layer, intermediate layer and loose layer. The dense layer was composed of Al_2TiO_5 and TiO_2 rutile phases, while the loose layer contained a large amount of amorphous SiO_2 besides Al_2TiO_5 and TiO_2 rutile phases.
(2) The maximum microhardness of MAO coating was about three times higher than that of TiAl substrate.
(3) The wearing rate of MAO coating was about 1/10 of TiAl substrate, and the microarc oxidation is a promising method to improve the wear resistance of TiAl alloy.
(4) By MAO surface treatment, the corrosion current density of TiAl substrate reduced about two orders of magnitude.

Acknowledgements

This research was supported by the National Natural Science Foundation of China (10575011) and the New-Star Program of Beijing Science and Technology Committee (9558102500).

References

[1] X. Li, S. Taniguchi, Y. Zhu, K. Fujita, N. Iwamoto, Y. Matsunaga, K. Nakagawa, Intermetallics 9 (2001) 443–449.
[2] Q. Yuan, C. Chi, Y. Su, Z. Xu, B. Tang, Trans. Nonferrous Met. Soc. 14 (3) (2004) 516–519.
[3] Zh.L. Tang, F.H. Wang, W.T. Wu, Surf. Coat. Technol. 99 (3) (1998) 248–252.
[4] A.L. Yerokhin, X. Nie, A. Leyland, A. Mathews, S.J. Dowey, Surf. Coat. Technol. 122 (1999) 73–93.
[5] V.S. Kulikauskas, E.A. Romanovsky, S.V. Semenov, I.V. Souminov, Nucl. Instrum. Methods Phys. Res. B 161–163 (2000) 553–557.
[6] W. Xue, Z.W. Deng, R.Y. Chen, T.H. Zhang, Thin Solid Films 372 (2000) 114–117.
[7] X. Nie, A. Leyland, H.W. Song, A.L. Yerokhin, S.J. Dowey, A. Matthews, Surf. Coat. Technol. 116 (1999) 1055–1060.
[8] S.V. Gnedenkov, O.A. Khrisanfova, A.G. Zavidnaya, S.L. Sinebrukhov, P.S. Gordienko, S. Iwatsubo, A. Matsui, Surf. Coat. Technol. 145 (2001) 146–151.
[9] L.A. Yerokhin, V.V. Lyubimov, R.V. Ashitkov, Ceram. Int. 24 (1) (1998) 1–6.
[10] W. Xue, C. Wang, R.Y. Chen, et al., Mater. Lett. 52 (2002) 435–442.
[11] S. Verdier, M. Boinet, S. Maximovitch, F. Dalard, Corr. Sci. 47 (2005) 1429–1444.
[12] Y.-K. Shin, W.-S. Chae, Y.-W. Song, Y.-Mo. Sung, Electrochem. Commun. 8 (2006) 465–470.
[13] W. Xue, C. Wang, Z. Deng, T. Zhang, ISIJ Int. 42 (2002) 651–655.
[14] Y. Wang, D. Jia, L. Guo, T. Lei, B. Jiang, Mater. Chem. Phys. 90 (2005) 128–133.
[15] X. Li, W. Xue, X. Wu, et al., Mater. Sci. Forum 546–549 (2007) 1769–1772.
[16] W. Xue, J. Du, X. Wu, Y. Lai, ISIJ Int. 46 (2006) 287–291.
[17] L. Rama Krishna, K.R.C. Somaraju, G. Sundararajan, Surf. Coat. Technol. 163–164 (2003) 484–490.
[18] S. Xin, L. Song, R. Zhao, X. Hu, Mater. Chem. Phys. 97 (2006) 132–136.
[19] W. Xue, Appl. Surf. Sci. 252 (2006) 6195–6200.
[20] T. Wei, F. Yan, J. Tian, J. Alloys Compd. 389 (2005) 169–176.
[21] X. Li, X. Wu, W. Xue, et al., Surf. Coat. Technol. 201 (2007) 5556–5559.